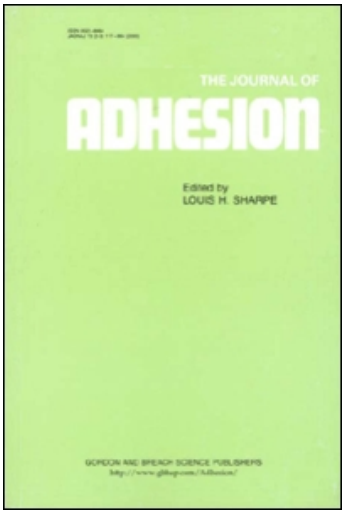

The Journal of Adhesion
Publication details, including instructions for authors and subscription information:
http://www.informaworld.com/smpp/title~content=t713453635

The Body's Response to Deliberate Implants: Phagocytic Cell Responses to Large Substrata *Vs.* Small Particles

R. Baier[a]; E. Axelson[a]; A. Meyer[a]; L. Carter[a]; D. Kaplan[b]; G. Picciolo[b]; S. Jahan[c]
[a] Department of Oral Diagnostic Sciences, State University of New York at Buffalo, Industry/University Center for Biosurfaces, [b] Food and Drug Administration, [c] University of Memphis,

To cite this Article Baier, R. , Axelson, E. , Meyer, A. , Carter, L. , Kaplan, D. , Picciolo, G. and Jahan, S.(2000) 'The Body's Response to Deliberate Implants: Phagocytic Cell Responses to Large Substrata *Vs.* Small Particles', The Journal of Adhesion, 74: 1, 79 — 101
To link to this Article: DOI: 10.1080/00218460008034525
URL: http://dx.doi.org/10.1080/00218460008034525

J. Adhesion, 2000, Vol. 74, pp. 79–101
Reprints available directly from the publisher
Photocopying permitted by license only

The Body's Response to Deliberate Implants: Phagocytic Cell Responses to Large Substrata *Vs.* Small Particles

R. BAIER [a,*], E. AXELSON [a], A. MEYER [a], L. CARTER [a], D. KAPLAN [b], G. PICCIOLO [b] and S. JAHAN [c]

[a]*State University of New York at Buffalo, Industry/University Center for Biosurfaces and Department of Oral Diagnostic Sciences;* [b]*Food and Drug Administration;* [c]*University of Memphis*

(Received 21 February 2000; In final form 30 October 2000)

It is important to characterize possible inflammatory responses to small particles, and to separate clearly these effects from responses to larger objects nearby. This research used a chemiluminescent assay, scanning electron micrographs, and energy dispersive X-ray spectra to monitor inflammation-related reactive oxygen intermediate (ROI) production and morphological alterations of human monocyte-derived macrophages interacting with the walls of apolar and polar polystyrene cuvettes, in the absence and presence of small particles of surface-characterized Teflon™, polyethylene, Co-Cr-Mo alloy, titanium and alumina. The two types of polystyrene substrata represent the "bacterial" (as produced) and "tissue culture" (gas-plasma-treated [GPT]) materials widely used in biological testing and tissue culture. Monocyte-derived macrophage spreading during contact with the higher-surface-energy, more polar substratum suppressed "oxidative bursts" to lower levels than expressed from rounded cells in contact with the lower-energy, apolar substratum. Particulate matter engulfed by both rounded and spread cells did not significantly enhance ROI production beyond levels observed for no-particle controls during the one-hour exposure time. Biocompatibility of some implants might be related to cell-spreading-induced suppression of ROI production, improving the tissue integration of GPT implants.

Keywords: Particles; Phagocytosis; Monocyte-derived macrophages; Reactive oxygen intermediates; Implants; Spreading; Chemiluminescence

*Address for correspondence: Industry/University Center for Biosurfaces, State University of New York at Buffalo, 110 Parker Hall, Buffalo, NY 14214-3007, USA. Tel.: 716-829-3560, Fax: 716-835-4872, e-mail: baier@acsu.buffalo.edu

INTRODUCTION

Medical and dental implants, their associated surgical placement debris, and loosened cement and wear debris particles all can be present simultaneously at sites of human prostheses. Even in the absence of infective microorganisms, inflammatory responses involving phagocytic cells often are associated with prosthetic hip, knee, and temporomandibular joint implants that show aseptic loosening [1]. This investigation set out to identify, using a simple *in vitro* model, the relative influences of engulfable small particles and of adjacent nonengulfable larger substrata on one early phase of phagocytic cell behavior: relative generation of reactive oxygen intermediates (ROI). The experiments simulated cases when biodegradation-resistant implants and biodegradation-resistant, engulfable particles would be simultaneously presented to arriving monocyte-derived macrophages. Human monocyte-derived macrophages were exposed to contact (10,000 cells per square centimeter) with reference polystyrene or gas-plasma-treated (GPT) polystyrene, serving as surrogate implant materials, while the monocyte-derived macrophages were allowed to contact and engulf small test particles (supplied at approximately 10 particles per cell) of titanium, cobalt/chromium/molybdenum alloy, Teflon, polyethylene, or alumina.

For 60 minutes after first "foreign materials" contact, monocyte-derived macrophage production of two key reactive oxygen intermediates, superoxide anion and hydrogen peroxide, was monitored in a luminometer assay developed by Kaplan and Picciolo [2]. In parallel experiments, scanning electron microscopy and energy-dispersive-x-ray analyses were used to monitor the changes in cell shapes and to confirm cellular engulfment and identity of test particles in each combined-contact experiment.

ROI production of human monocyte-derived macrophages was most strongly correlated ($p < .001$) with their spread areas in contact with the nonengulfable (cuvette walls or separate test specimens) substrata, suggesting that (a) variable cell spreading might trigger variable cell-membrane-based configuration changes of catalytic macromolecules known to be important in the early inflammatory responses of phagocytes [3–5], or (b) ROI was not detectable by the probe due to sequestration.

MATERIALS AND METHODS

Human Cells

Monocyte-derived macrophages were prepared and used in the morphological and oxidative studies, in accord with detailed protocols previously published [6]. Monocytes were isolated from adult humans by leukophoresis. The cell population was enriched for monocytes by elutriation. The cells were cultured in polypropylene tubes for 3-8 days in the presence of M-CSF (macrophage colony stimulating factor) and human AB serum to differentiate the monocytes to monocyte-derived macrophages [6]. Half the media were changed every other day.

Test Substrata

The nonengulfable substrata utilized in this study were reference polystyrene (PS) and gas-plasma-treated polystyrene (GPTPS), both previously characterized in detail with regard to their utility and properties for cell adhesion experiments [7]. For the cell contact studies, these materials were used in a flat, sheet form. For the oxidative studies, these materials were in a cuvette form allowing easy use in the luminometer assay [2].

Test Particles

Five types of implant-relevant, engulfable particles were used, first prepared in dry form as powder-like materials. Three types were gifts from Smith Nephew Orthopedics (Memphis, TN) including ASTM F-75 (Co-Cr-Mo), high density polyethylene (HDPE) and titanium, which are referred to herein as F-75, PE and Ti, respectively. These materials were represented to be relevant to orthopedic industry interests in biological responses to wear debris near articulating segments of orthopedic implants, including the total joint replacement implants of the hip and knee [8]. Alumina was a gift from Ivoclar North America, as representative of the material widely used to surface-abrade many implant materials and found embedded in implant surfaces [9]. Impact-fractured Teflon (Tef) was used, from a

supply first prepared to assess phagocytic responses in the chick chorioallantoic membrane model [10]. Teflon particulate is clinically relevant, since Teflon wear debris from failed temporomandibular joint implants has been implicated as a causative agent in stimulating and sustaining inflammatory reactions that led to implant rejection [11]. Multisizer data and scanning electron microscope images showed that all the test particles were between $1-10\,\mu m$, a range suitable for particle internalization by monocyte-derived macrophages (phagocytosis).

Particle/Monocyte-derived Macrophage Exposure Experiments

Approximately 50 million monocyte-derived macrophages in 1 mL of prepared complete medium (FBS, human AB serum, M-CSF, glutamine, glucose) were prepared by a 10x dilution with complete medium and stored at room temperature. Reference and GPT polystyrene specimens were individually placed in labeled dishes. Milligram quantities of particles of each type were placed on separate pieces of reference and GPT polystyrene. With a glass pipette, approximately $500\,\mu L$ of cell suspension was aliquoted and carefully applied to each particle type. Pipetting up and down formed suspensions in which cell-particle contacts were maximized. These suspensions then were re-applied to the original GPT or reference polystyrene substrata, in approximately $150\,\mu L$ drops. "No-particle" control specimens were included in each test series and were treated in the same manner as cells + particles samples. The samples were covered and incubated at 37°C for 1 hour to allow for cell attachment and spreading over the substratum and concurrent phagocytosis of the particles. After 1 hour, liquid was removed from each drop-covered area with a glass pipette, and the remaining substrata with attached cells and particles were processed for SEM by fixation in 2.5% glutaraldehyde (GA), followed by dehydration in a graded series of ethanol/water mixtures, and critical-point drying from hexamethyldisilazane (HMDS). The GA, ethanol/water mixtures, and HMDS were applied in sequential drop-wise fashion over the original cell- and particle-exposed areas.

Scanning Electron Microscopy/Energy Dispersive X-ray (SEM/EDX) Analysis

Samples were further processed for SEM/EDX by mounting the drop-exposed, fixed specimens on aluminum stubs with double-sided, conductive carbon tape. The specimens then were overcoated with sputtered carbon. SEM images and EDX spectra were recorded for substrata, cells, and particles. Most SEM images were collected at 20 keV acceleration voltage and EDX spectra were collected at 100,000x magnification (100 kx). Additional SEM images and EDX spectra were collected at 3 keV acceleration voltage to resolve better the cell and particle morphology. SEM images of a 10 μm diffraction grating were used to calibrate the magnification scales for quantitative analyses of the shape parameters of attached monocyte-derived macrophages, including cell diameter and surface area, on the GPT *versus* reference polystyrene substrata.

Particle Stocks

Test particle suspensions of 25 mg/mL in physiologic saline were prepared. High-speed vortexing was used to create homogeneous suspensions prior to addition to the test cuvettes.

Particle counts were obtained using a Coulter Counter (Beckman Coulter, Inc., Fullerton, CA) equipped with a 50 μm diameter aperture and software capable of generating particle size distribution curves from the recorded counts. Prior to counting, each particle stock was vortexed and 100 μL of the suspension was added to 20 mL of particle-free Isoton balanced electrolyte solution (Coulter) and counted in triplicate. The polyethylene and Teflon particle stock suspensions were unstable, as the intrinsic hydrophobicities of the particles caused clumping in the aqueous fluid. The alumina particles settled faster than did the titanium and cobalt-chromium-molybdenum particles after votexing. These difficulties were overcome by introducing pre-weighed, pre-dispersed amounts of PE, Teflon, and alumina particles to the experimental cuvettes, after determining the amounts necessary (about 10 particles per cell) to best utilize the operating range of the luminometer instrument.

Measurements also were made of particle-induced changes in contact angles and in the surface tensions of standard diagnostic liquids [12], as well as noting the liquid surface tensions associated with spontaneous particle engulfment. Contact angles of single drops of various diagnostic liquids of known surface tension first were measured as these drops rested at equilibrium upon reference-grade PTFE (polytetrafluoroethylene) film. Test particles were added in dry form to the various drops by simply sprinkling them over the drops. After addition of particles, drop contact angles were again measured while the drops were viewed through a 10x telescope for observations of particle engulfment or particle exclusion to the external surface of the drop.

IR spectra were acquired for the test particles and their extracted "residues" as dried from distilled water slurries on germanium prisms. Testing for the presence of endotoxins associated with the particles was done by a commercial Limulus Amoebocyte Lysate (LAL) *in-vitro* test.

Processing Monocyte-derived Macrophages for the Chemiluminescent (CL) Assay

Stock cells, in complete medium, were taken from a supply kept rotating in an incubator at 5% CO_2 and 37°C, within 2 days of their donation. Prior to CL assay, the cells were pelleted by gentle centrifugation (2000 rpm, approximately 250x g) for 10 minutes, to remove the supernatant and thereby minimize the contribution of medium components (*e.g.*, serum) to the measurements. Diluting medium supplemented with salts and glucose was used to resuspend the pellet. Pipetting up and down, as in the particle contact trials, and additional vortexing, fully dispersed the cells and created homogeneous suspensions. Cells used for control experiments were processed by all the steps outlined above. The numbers of viable cells present were determined by using a standard hemocytometer and 100 μL aliquots of the cell suspensions (cells stained with Trypan blue). Net viable cells were determined as the difference between total cells present and those colored blue (dead or dying).

Prior to the CL assay, test particles were placed in the luminometer cuvettes and suspended in 100 μL of diluting medium and 750 μL of

luminescent "probe". Cuvette exteriors were wiped with a lint-free cloth (pre-wetted with anti-static solution) and loaded into the luminometer according to a "run list" specified in the software. Cells from stock suspensions (5×10^5 viable cells per ml) then were added to the cuvettes in 100 µl aliquots with a repetition pipettor, so that each luminometer cuvette contained 5×10^4 cells (final concentration: 5.26×10^4 cells/ml). Preliminary experiments indicated that this concentration of cells resulted in a linear CL response; no oxygen diffusion problems were noted. The door of the apparatus was closed to initiate the data collection program. The luminometer program repeatedly analyzed 25 tubes every 4 minutes, shaking each individual sample prior to its reading. Data collection was stopped after 1 hour, at the completion of the nominal "inflammatory phase" [6]. Although one hour is a very short time, in terms of host response and longer-term biocompatibility of implants, the experiments reported here were designed to indicate the *potential* for the test substrata and particles to initiate an inflammatory response. Further validation of the CL assay as a predictive tool is underway at this time.

Chemiluminescent (CL) Assay Conditions and Reagents

With reference polystyrene luminometer cuvettes, suspensions of 1, 10, and 100 particle(s) per monocyte were tested in a series of preliminary experiments. It was determined that the best use of the instrument's experimental range was for about 10 particles/cell; this proportion was used in all subsequent assays. Slight turbidity was noted only for the experiments with titanium particles. Measurements indicated that chemiluminescence could be diminished by as much as 5% by the turbidity caused by the titanium particles, if the particles stayed in suspension. The data related to titanium that are presented in this report are not corrected for turbidity, as an accurate and reproducible correction factor could not be obtained. Commercially-supplied lucigenin and luminol reagents were used to assess superoxide anion (O_2^-) and hydrogen peroxide (H_2O_2) production, respectively. Cuvettes pre-coated with a known tumorigenic phorbol ester (phorbol myristate acetate (PMA)) were used as positive controls, typically inducing generation of reactive oxygen intermediates at 3–5 times the

amount noted for uncoated cuvettes. The reagent suspensions in reference and GPT polystyrene luminometer cuvettes without particles served as cuvette controls. Experiments were performed in triplicate.

Electron spin resonance measurements of reference PS and GPTPS, to estimate free radicals, were performed in accord with a method used to examine radiation-sterilized artificial hip components [13].

Cell Viability Using Probes

The apparent cytotoxicities of the test particles at the contact conditions used in the chemiluminescent assays were determined by using commercially-supplied calcein and ethidium probes. Cell viability was microscopically assessed after exposure to particles at concentrations and exposure times similar to those in the corresponding CL assay. Green (viable, calcein) and red (dead, ethidium bromide) cells were microscopically visualized, manually counted and videotape-recorded in five separate fields per chamber and in three separate modes including transmitted light (all cells), calcein mode, and ethidium bromide mode by adjusting filters on a bright field microscope.

Data Reduction Techniques

The CL responses for luminol and lucigenin were measured as the mean integral light emission for each sample monitored, using the instrument's automatic calculation of the area under the light emission curve. Percent variance (% variance) of 5–10% for data in triplicate was typical.

RESULTS

Cell Viability

Results from cell viability assays using calcein and ethidium bromide probes showed the Ti particles to cause between 43 and 69% cytotoxicity. F-75 particles were cytotoxic at levels between 8% and 48%. The alumina showed 0 to 25% cytotoxicity.

Teflon showed 0–31% cytotoxicity, and PE particles were 6–27% cytotoxic according to these assays.

Endotoxin Testing

The Teflon particles carried endotoxin at the level of 48 EU (standard units), compared with 0.06 EU or less for all the other test particles.

Production of Reactive Oxygen Intermediates

The differential oxidative responses of monocyte-derived macrophages are recorded in Figures 1 and 2 for cells contacting reference *versus* gas-plasma-treated polystyrene, alone, and as challenged with additions of engulfable test particles in identically-prepared cuvettes. With the exception of titanium, superoxide anion production was not enhanced by any other of the test particles. ANOVA analysis of the data demonstrated that gas-plasma-treatment (GPT) of polystyrene significantly reduced polystyrene's ability to elicit a superoxide production response from monocyte-derived macrophages, as shown in Figure 1 ($p < .001$) and Figure 2 ($p < .05$). This reduction in superoxide production response in GPTPS also was observed, at the same levels of significance, for specimens with added particles.

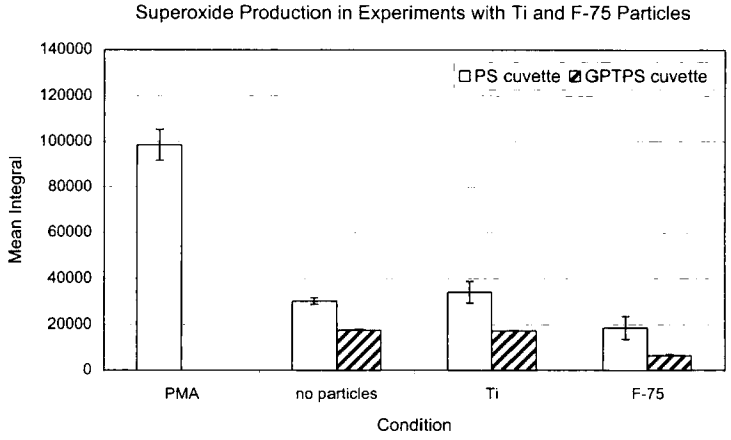

FIGURE 1 The superoxide production of human monocyte-derived macrophages exposed to the Ti and F-75 test particles in GPT surface-modified and control cuvettes using lucigenin as the CL probe (note: 10 particles/cell introduced; $\sim 1 \times 10^4$ cells/cm^2 cuvette surface; average $\pm$ standard deviation of triplicates; PMA = phorbol ester positive control). Response of cells in GPTPS cuvettes was significantly less ($p < .001$) than cells in control cuvettes.

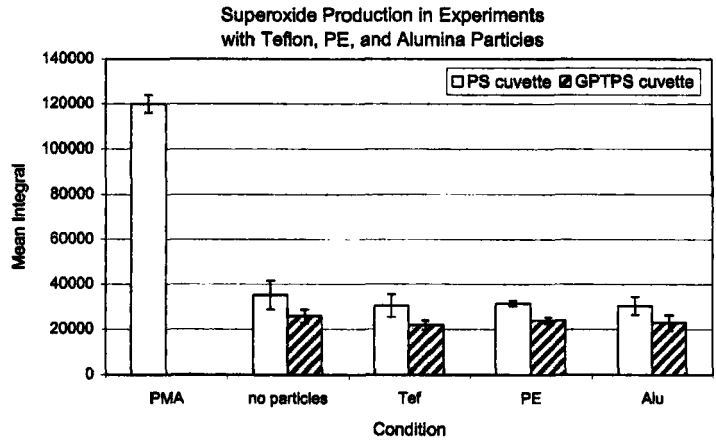

FIGURE 2 The superoxide production of human monocyte-derived macrophages exposed to the PE, Teflon, and alumina test particles in GPT surface-modified and control cuvettes using lucigenin as the CL probe (note: 2 mg introduced; $\sim 1 \times 10^4$ cells/cm^2 cuvette surface; average $\pm$ standard deviation of triplicates; PMA = phorbol ester positive control). Response of cells in GPTPS cuvettes was significantly less ($p < .05$) than cells in control cuvettes.

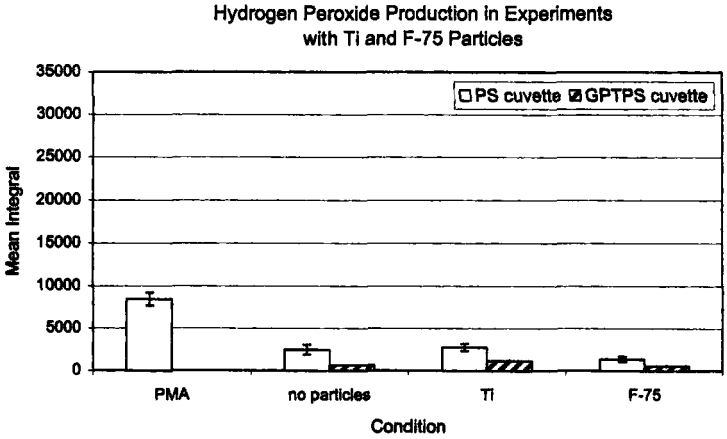

FIGURE 3 The hydrogen peroxide production of human monocyte-derived macrophages exposed to the Ti and F-75 test particles in GPT surface-modified and control cuvettes using luminol as the CL probe (note: 10 particles/cell introduced; $\sim 1 \times 10^4$ cells/cm^2 cuvette surface; average $\pm$ standard deviation of triplicates; PMA = phorbol ester positive control). Response of cells in GPTPS cuvettes was significantly less ($p < .001$) than cells in control cuvettes. Ti particles were slightly stimulatory above the reference PS control ($p < .05$).

Results for the hydrogen peroxide production response of human monocyte-derived macrophages are recorded in Figures 3 and 4. Although the Ti and alumina particles were slightly stimulatory above the reference PS control value ($p < .05$ and $p < .001$, respectively), F-75, Teflon and PE particles did not activate the cells beyond that of the reference PS. As with the superoxide cell response, contact with GPTPS reduced the ability of the cells to produce a hydrogen peroxide response; this effect also was observed for all of the particle-added cases ($p < .001$ in all cases). Table I presents data confirming that the GPT effect is a general feature of gas-plasma-induced surface energy changes for the PS, and not specific to the gas used (argon *vs.* air). Two-tailed Student t-tests demonstrated no significant differences between the two methods of gas plasma treatment evaluated in the preliminary experiments. Electron spin resonance results showed that GPT-induced superficial free radicals were present on the PS, but decayed to 75% of initial levels before the cell contact experiments were performed (Tab. II).

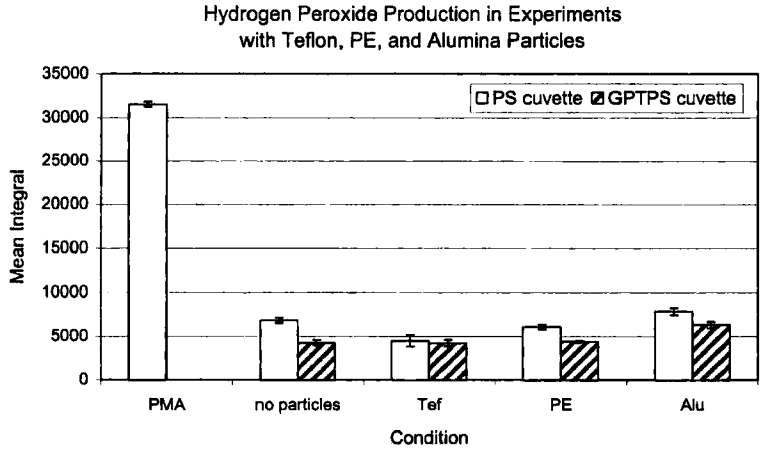

FIGURE 4 The hydrogen peroxide production of human monocyte-derived macrophages exposed to the PE, Teflon, and alumina test particles in GPT surface-modified and control cuvettes using luminol as the CL probe (note: 2 mg introduced; $\sim 1 \times 10^4$ cells/cm^2 cuvette surface; average $\pm$ standard deviation of triplicates; PMA = phorbol ester positive control). Response of cells in GPTPS cuvettes was significantly less ($p < .001$) than cells in control cuvettes. Alumina particles were slightly stimulatory above the reference PS control ($p < .001$).

TABLE I The hydrogen peroxide production of human monocyte-derived macrophages exposed to the Ti test particles in air- and argon-plasma-treated and control cuvettes using luminol as the CL probe (note: 10 particles/cell introduced; $\sim 1 \times 10^4$ cells/cm^2 cuvette surface, (+) = air-plasma-treated; (R+) = argon-plasma-treated). There is no significant difference between results from the two methods of gas plasma treatment

Luminol response for Ti in air vs. argon-plasma-treated PS cuvettes (Hydrogen Peroxide Production from Human Monocyte-derived Macrophages)

Sample	*Mean integral values*	*% coeff. variance*
PMA	23,736	14.5
PS	3,882	12.6
PS+	2,498	10.0
PS-R+	2,454	6.5
Ti	6,407	3.9
Ti+	3,605	12.2
Ti-R+	3,559	8.2

TABLE II Relative free radical concentration in gas-plasma-treated polystyrene stored in air under ambient laboratory conditions. Data represent peak-to-peak height of signal in electron spin resonance spectra

ESR signal reduction during 72 hours after gas plasma treatment of polystyrene

Post-GPT time (hours)	*Peak-to-peak height*	*Interval decay rate [units/hour]*
Time zero	44.15	–
1.5	44.76	–
6.5	39.18	1.12
24.5	37.65	0.09
72.0	32.87	0.10
No-GPT control	no detectable signal	–

Cell Morphology and Chemistry Changes

SEM images of human monocyte-derived macrophages on reference polystyrene substrata, after one-hour contact times, showed typical cells to be roughly spherical, but attached at multiple substratum sites with small surface membrane "retraction filaments" at their bases (Fig. 5). In contrast, SEM images of monocyte-derived macrophages from the same source, allowed to contact GPTPS substrata for one hour, showed these cells to be very flat and to have very close membrane association with the GPT substratum (Fig. 6). Cell diameters on the reference polystyrene were 8.8 μm ± 0.4 μm, and 18.0 μm ± 0.5 μm on the GPTPS. The apparent cell surface/substratum contact areas

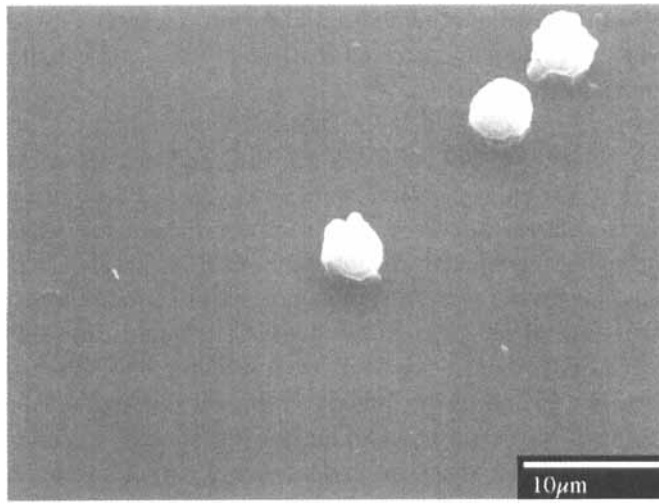

FIGURE 5 SEM photomicrograph of monocyte-derived macrophage on reference polystyrene after one hour contact. Note absence of cell spreading. Original magnification: 2000x.

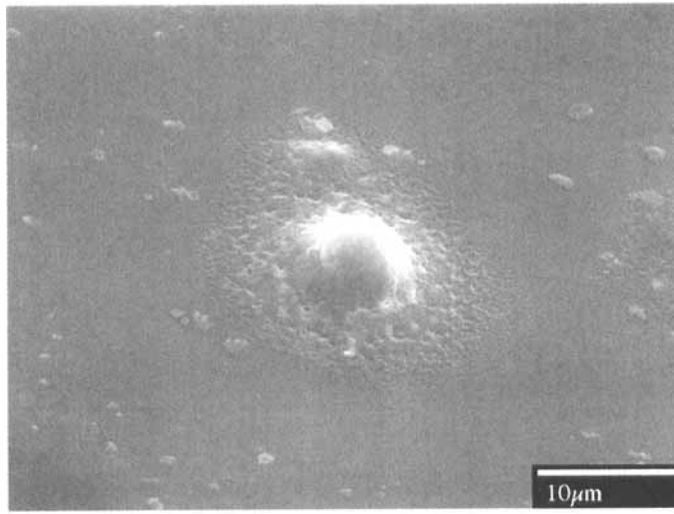

FIGURE 6 SEM photomicrograph of monocyte-derived macrophage on GPT polystyrene after one hour contact. Note spread membrane-bound cytoplasmic "skirt" which extends approximately 10 μm from the prominent nucleus of the cell. Original magnification: 2000x.

were $240\,\mu m^2 \pm 20\,\mu m^2$ and $950\,\mu m^2 \pm 50\,\mu m^2$, respectively. A two-tailed Student t-test demonstrated that the difference in cell diameters was significant ($p < .001$).

EDX spectra of cells on the reference PS contained characteristic biological salt-related peaks for Na, Cl, P, O and to a lesser extent, K and Ca (Fig. 7). These elements were absent from PS not exposed to cells and from areas of cell-exposed samples without cell attachment. A strong signal for Si also was noticed from EDX spectra of the supplied cells, suggesting some silica fine particle contamination from the elutriation and related preparative steps. Cells retained on GPT substrata similarly contained Na, Cl, P, O, K, Ca and Si, with accentuated signals for Na, Cl and Si, attributed to media residues retained around the spread cells on intrinsically polar (more wettable) specimens [14].

When test particles also were present, many particles were observed to be in close physical association with monocyte-derived macrophages (Fig. 8). Cells having attached or engulfed the various particles usually showed irregular topographical appearances but did not

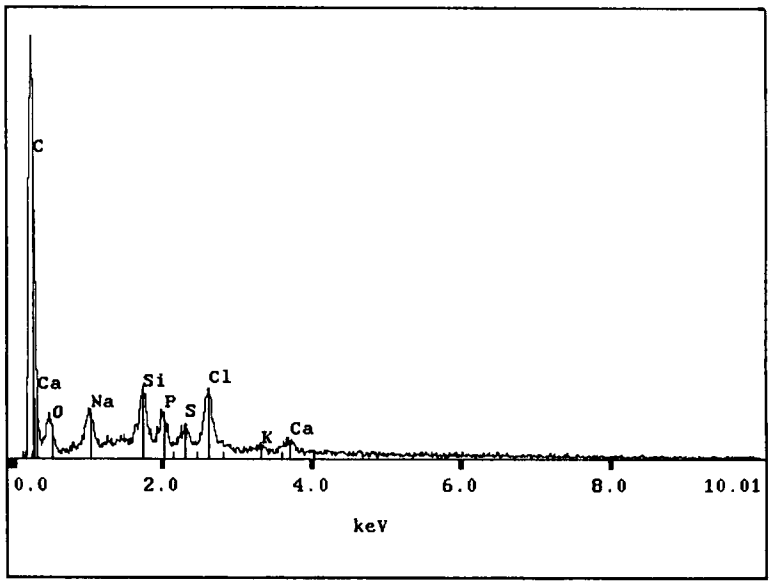

FIGURE 7 Energy-dispersive X-ray spectrum of monocyte-derived macrophages on reference polystyrene. Except for carbon, other detected elements are attributed to salts from medium.

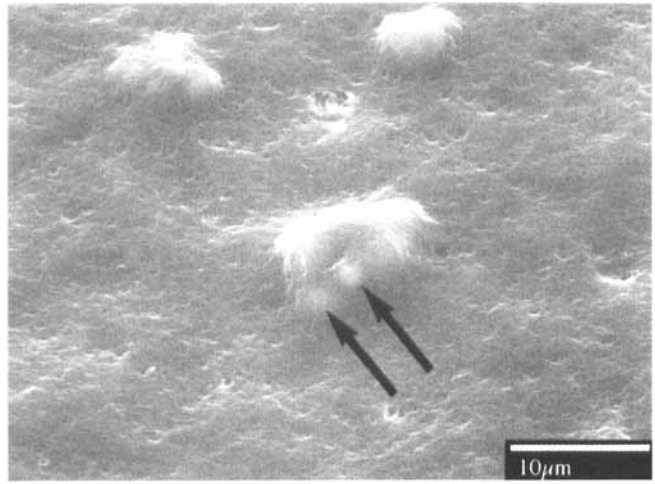

FIGURE 8 SEM photomicrograph of cells and engulfed F-75 particles (arrows) on GPTPS. Original magnification: 2000x.

change from their substratum-specific initial spread cell areas. Some irregular cell perimeters resulted from cell membrane attachments to nearby particulate matter (Fig. 9). These appeared to be mainly

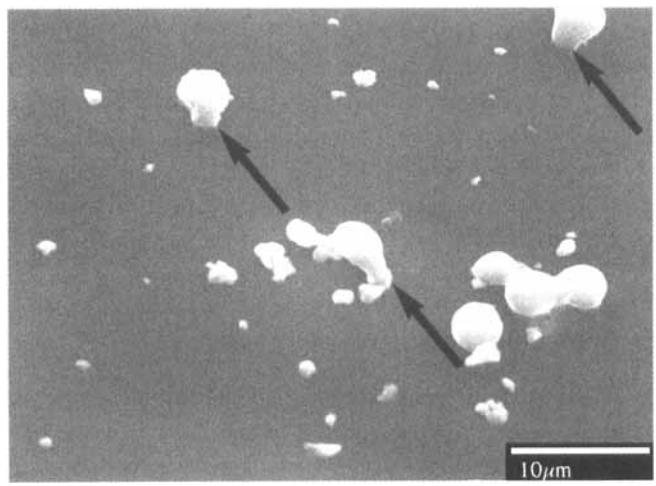

FIGURE 9 Irregular cell perimeters were observed when the cell membrane remained attached to nearby particulate matter (arrows). In the example, cells are on reference PS, and are contacting alumina particles. Original magnification: 2000x.

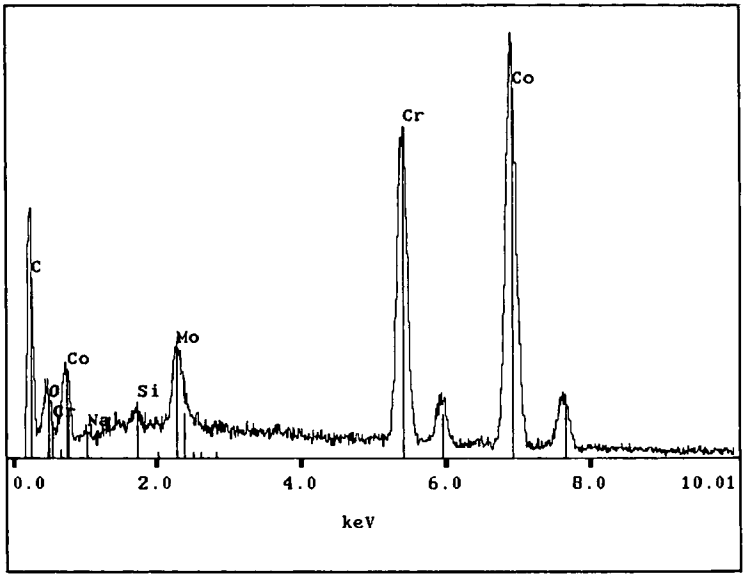

FIGURE 10 EDXray spectrum of F-75 particles engulfed by cell shown in Figure 8.

retraction fibers, and were more prominent when the higher-energy particles were on the intrinsically less adhesive (less cell spreading) reference polystyrene [15].

The various particles could be readily chemically identified, inside and outside cell bodies by using EDX spectra, with alumina, Ti, F-75, Teflon, and PE showing characteristic peaks of Al, Ti, Co-Cr-Mo, F and C, respectively. Figure 10 is an EDXray spectrum from F-75 particles within the central region of a well-spread monocyte-derived macrophage on GPTPS (see SEM photomicrograph, Fig. 8).

Surface Characteristics of Test Particles

Each dry particle preparation diminished the initial contact angles of some diagnostic liquids, first placed as drops on reference PTFE film, indicating that trace, leachable, surface-active contaminants were present in all preparations. Table III is a typical data set, in this case for the Teflon particles. Except for the F-75 particles, all the other

TABLE III The particle-induced changes in contact angles and point of initial engulfment for the Teflon test particles. Values in italics indicate leachable, surface-active contaminants on particles

Teflon particle-induced changes in contact angles on reference PTFE film and point of initial engulfment

Reference liquid	*Surface tension (dynes/cm)*	*Average initial contact angle (°)*	*Average final contact angle (°)*	*Engulfment (yes/no)*
Water	72.0	114, 116	116, 111	N
Glycerol	65.0	111, 110	*105, 103*	N
Formamide	58.0	105, 103	*85, 86*	N
Thiodiglycol	53.5	104, 106	*89, 89*	N
Methylene Iodide	49.0	85, 89	*82, 81*	N
1-bromo Naphthalene	45.0	81, 83	83, 80	N
Methyl Naphthalene	39.0	78, 80	*75, 72*	N
Dicyclohexyl	33.0	68, 69	*54, 55*	N
Hexadecane	27.5	47, 48	*20, 20*	N
Decane	24.0	35, 33	*25, 25*	N

particles behaved as could be predicted from their nominal critical surface tensions with regard to their spontaneous engulfment or exclusion from the various diagnostic liquids. Teflon particles, with nominal critical surface tension of about 18 dynes/cm, were insufficiently "wetted" by any of the diagnostic liquids to be engulfed into the liquid drops (see Tab. III). PE particles, with nominal critical surface tension in the mid-30's dynes/cm, were engulfed by methylnaphthalene, suggesting that the surface zone of these particles was probably oxidized during the preparative steps, as occurs with polyethylene cups for artificial hips [13]. Alumina and titanium particles, nominally of high critical surface tensions, were spontaneously "wetted" and engulfed by all the diagnostic liquids. F-75 particles, from cobalt-chromium-molybdenum alloy with a nominally high critical surface tension, were excluded from diagnostic liquids of high surface tension, but were engulfed by liquids having surface tensions of 33 dynes/cm or less. These wettability data show that the F-75 particles were coated with a low-surface-energy substance, probably similar to typical organic-polish-contaminated Co-Cr-Mo surfaces of fabricated medical devices [16, 17].

Infrared (IR) spectra for the Ti particles, dried from a distilled water slurry, showed no significant absorption bands above baseline, indicating that any water-leachable contaminant associated with these particles was present in very small quantities. For the Teflon particles, dried from a distilled water slurry, only the carbon-fluorine peaks around $1200\,cm^{-1}$ were evident, confirming the identity of this polymer, but providing no additional compositional evidence about the endotoxins present. The F-75 particles, also dried from a distilled water slurry, did not show any elutable organic contamination in their IR spectra; recall that no significant *leachable* surface-active material was detected from the contact angle analyses. IR spectra for the alumina particles, dried from a distilled water slurry, had a broad peak centered at $3400\,cm^{-1}$, and sharper peaks at 1650 and $1375\,cm^{-1}$, indicating the presence of a hygroscopic salt (probably a carbonate) contamination phase. The PE particle spectrum revealed both the characteristic absorbance bands for hydrocarbons, two between 2800 and $2900\,cm^{-1}$ and two around $1400\,cm^{-1}$, and a broad band at $3400\,cm^{-1}$ consistent with partial surface oxidation of the PE particles.

DISCUSSION

Exposure to implantable medical device materials and any associated particles resulting from wear or biodeterioration can elicit an oxidative burst from phagocytes of the immune surveillance system. Reactive oxygen intermediates (ROI), which are usually generated during phagocytic events, might vary in amounts produced and have different material-dependent consequences for tissue compatibility and inflammation. Prior studies showed that both phagocytic and ROI responses are surface-contact and adhesion dependent [1]. Although it also has been shown that macrophages exhibit variable morphological changes upon contact with chemically-diverse substrata [18, 19], no prior work has actually discriminated between the separate and combined influences of large-area biomaterial substratum surface chemistry and small debris particles, which might be simultaneously present at an implant location. This research used a chemiluminescent (CL) assay, scanning electron micrographs (SEM), and energy dispersive x-ray

spectra to document the ROI production and morphological alterations of monocytes interacting concurrently with characterized small particles of Teflon, polyethylene, Co-Cr-Mo alloy, titanium, and alumina on two characterized polystyrene substrata ("bacterial"-grade and "tissue culture"-grade) [7]. The relative ROI production associated with these interactions was monitored by an oxidative burst assay [2]. Considered together, the SEM and CL assay results showed significantly greater ($p < .001$) monocyte-derived macrophage spreading upon contact with higher-surface-energy substrata (GPTPS), which significantly suppressed ($p < .001$ in most cases; $< .05$ in all cases) the "oxidative burst" observed when lower-energy substrata of the same bulk composition (PS) were contacted. Concurrent presence of particulate debris had little additional influence. Slightly more ROI was produced in the presence of titanium or alumina particles ($p < .05$), relative to the no-particle controls.

Formation of oxygen-derived free radicals by various phagocytes (neutrophils, eosinophils, monocytes, and macrophages) is catalyzed by a membrane-bound enzymatic complex, the NADPH oxidase, which is dormant in resting cells, but becomes activated during surface contact, phagocytosis or following interaction of the cells with suitable soluble stimulants [3]. This respiratory burst oxidase of phagocytes catalyzes the one-electron reduction of molecular oxygen by NADPH to form superoxide anion (O_2^-), the precursor of a number of other reactive oxidants that function as microbicidal agents [4, 5].

In addition to the NADPH oxidase, several other enzymes in phagocytes are key to controlling contact-induced ROI production, including superoxide dismutase (SOD) [20, 21], catalase and myeloperoxidase (MPO) [22]. Superoxide is dismutated to hydrogen peroxide spontaneously or by SOD. Hydrogen peroxide is further reduced to hydroxy radical *via* the iron-catalyzed Haber-Weiss reaction, in which ferrous iron (Fe^{2+}) reduces H_2O_2 to form hydroxy radical ($\cdot OH$) and hydroxide ion (OH^-). The reactive oxygen intermediates produced by phagocytes are responsible for maintaining pathogen-free environments as a part of the normal host defense mechanism, but can also pathologically mediate cell injury during activation. Current evidence concerning the mechanisms of cell injury by activated oxygen species suggests that O_2^- and H_2O_2 injure cells as

a result of the generation of more potent oxidizing species [23]. It is thought that O_2^- reduces a cellular source of ferric to ferrous iron, which reacts with H_2O_2 to produce the known more potent oxidizing species, hydroxy radical ($\cdot OH$), that can then initiate the peroxidative decomposition of the phospholipids of cellular membranes, damage the inner mitochondrial membrane, or oxidatively damage DNA [23].

The biological consequences of particulate wear debris associated with implants have been related to many factors of both the particulate and bulk material, including material composition, size, shape, surface area, density and surface topography [1, 24, 25]. The rate of production of the particulate, relative to the number of phagocytes present, also may determine the extent of the biological response.

One explanation for the clear division of results obtained here, between the reference PS and GPTPS substrata groups, is that the altered chemistry of the GPTPS surface, with a surface polarity notably higher and most similar to "tissue culture" polystryene (also produced by a GPT process), was more effective in sustaining intimate contact with the cell-surface membranes. Distortion of the plasma membranes by spreading and tension could have impaired the ability of the membrane-associated NADPH oxidase to catalyze ROI production. Another explanation is that ROI was produced and was either sequestered or dissipated within the cell/substratum pocket and, thus, was unavailable to the CL probe. Other methods do exist for measuring reactive oxygen intermediates [26–31] and should be pursued in future studies.

CONCLUSIONS

These data show that modulation of monocyte-derived macrophage production of reactive oxygen intermediates (ROI), including superoxide anion (O_2^-) and hydrogen peroxide (H_2O_2), was more dependent on the contact surface properties of the large unbroken substrata surfaces than on the types of particles these cells contacted and engulfed during the first hour of exposure. This was the case for monocyte-derived macrophages in contact either with reference or gas-plasma-treated polystyrene and any of 5 types of potential

implant-related wear particles (titanium, cobalt-chromium-molybdenum alloy, Teflon, polyethylene, and alumina). Specifically, cell contact with gas-plasma-treated polystyrene (GPTPS) suppressed the human monocyte-derived macrophage release of superoxide anion and hydrogen peroxide to amounts approximately 40% of those produced by identical cell contact with reference polystyrene ($p < .05$). The concurrent morphological consequence of cell contact with GPTPS was spontaneous cell spreading to about four times the surface area noted for monocyte-derived macrophages attached to reference PS. Since particle engulfment was confirmed by microscopy and elemental analysis for the monocyte-derived macrophages in both instances, differential cell spreading did not impair the events of phagocytosis but did modulate reactive oxygen generation. Or, if ROI was generated and sequestered, differential cell spreading modulated detection of the ROI by the CL probe.

Titanium particles showed slight enhancement of ROI production by monocyte-derived macrophages in contact with both reference and GPTPS, associated with loss of cell viability. Endotoxin contamination of the test particles to amounts less than 50 EU/mL did not increase ROI production or cell spreading on nonengulfable substrata. Variations of surface hydrophobicity, hydrophilicity, or apparent critical surface tension of the particles were of minor influence on monocyte-derived macrophage ROI production and morphology. Much greater during the one-hour exposure period were the influences of modification of the unbroken polystyrene surface properties from low-to high-surface-energy.

Polystyrene substratum surface energy modifications produced by GPT in argon gas and in air, and in different GPT devices, resulted in increased cell spreading and decreased ROI production by contacting monocyte-derived macrophages. These results reflect the relatively permanent changes in the surface energy state of GPTPS, persisting for long times beyond the independently documented decay of GPT-induced surface free radicals [7, 13, 15]. Suppression of "inflammatory" ROI bursts, by GPT-induced surface energy and surface polarity increases, may explain superior implantation results found for GPT prosthetics [32-34]. Follow-up experiments with flat coupons of untreated and GPT implant materials (*e.g.*, Ti, F-75, PE) in the absence of particles are planned.

Acknowledgment

The authors are grateful to Dr. Thomas Nicotera of the Roswell Park Cancer Institute, Buffalo, NY, for expert advice on reactive oxygen intermediate species.

References

[1] Carter, L. C., *Handbook of Biomaterials Evaluation* (Taylor & Francis, Philadelphia, 1999), 2nd edn., Chap. 14, pp. 241–252.
[2] Kaplan, D. S., Picciolo, G. P. and Mueller, E. P., *U.S. Patent* **5**, 294, 541 (1994).
[3] Bellavite, P., *Free Radic. Biol. Med.* **4**, 225 (1988).
[4] Babior, B. M., *Environmental Health Perspectives* **102**, 53 (1994).
[5] Johnston, R. B., *Fed. Proceedings* **37**, 2759 (1978).
[6] Picciolo, G. L., Kaplan, D. S., Kapur, R., Rudolph, A. S., Dulcey, C. S. and Tamerius, J. D., *Cells and Materials* **6**, 291 (1996).
[7] Baier, R. E., Rittle, K. H. and Meyer, A. E.,*Principles of Cell Adhesion* (CRC Press, Boca Raton, 1995), Chap. 2, pp. 41–62.
[8] Clarke, I. C. and McKellop, H. A., *Handbook of Biomaterials Evaluation* (Macmillan, New York, 1986), Chap. 10, pp. 114–130.
[9] Flynn, H. E., Natiella, J. R., Meenaghan, M. A. and Carter, J. M., *J. Prosthetic Dent.* **48**, 82 (1982).
[10] Carter, L. C., Analysis of the Cellular Healing Response of the Chick Chorioallantoic Membrane to Implanted Poly(Glycolic) Acid. *Doctoral Thesis.* State University of New York at Buffalo (1993).
[11] Hensher, R., *Brit. J. Hosp. Med.* **53**, 455 (1995).
[12] Baier, R. E., Gott, V. L. and Feruse, A., *Trans. Amer. Soc. Artif. Int. Organs* **XVI**, 50 (1970).
[13] Jahan, M. S., Thomas, D. E., Banerjee, K., Trieu, H. H., Haggard, W. O. and Parr, J. E., *Radiation Phys. and Chem.* **51**, 593 (1998).
[14] Baier, R. E., *Adsorption of Microorganisms* (Wiley-Interscience, New York, 1980), pp. 59–104.
[15] Rittle, K. H., Influence of Surface Chemical Factors on Selective Cellular Retention. *Doctoral Thesis.* State University of New York at Buffalo (1991).
[16] Baier, R. E., Gott, V. L. and Dutton, R. E., *J. Biomed. Mater. Res.* **6**, 465 (1972).
[17] Carter, J. M., Flynn, H. E., Meenaghan, M. A., Natiella, J. R., Akers, C. K. and Baier, R. E., *J. Biomed. Mater. Res.* **15**, 843 (1981).
[18] Anderson, J. M., *Trans. Amer. Soc. Artif. Int. Organs* **34**, 101 (1988).
[19] Lohmann, C. H., Schwartz, Z., Koster, G., Jahn, U., Bochhorn, G. H., MacDougall, M. J., Casasola, D., Liu, Y., Sylvia, V. L., Dean, D. D. and Boyan, B. D., *Biomaterials* **21**, 551 (2000).
[20] McCord, J. M. and Fridovich, I. J., *Biol. Chem.* **244**, 6049 (1969).
[21] Salin, M. L. and McCord, J. M., *J. Clin. Invest.* **54**, 1005 (1974).
[22] Robinson, P. J. and Babcock, G. F., *A Guide for Research and Clinical Evaluation* (Wiley-Liss, New York, 1998).
[23] Farber, J. L., *Environmental Health Perspectives* **102**, 17 (1994).
[24] Shanbhag, A. S., Jacobs, J. J., Black, J., Galante, J. O. and Glant, T. T., *J. Biomed. Mater. Res.* **28**, 81 (1994).
[25] Voronov, I., Santerre, J. P., Hinek, A., Callahan, J. W., Sandhu, J. and Boynton, E. L., *J. Biomed. Mater. Res.* **39**, 40 (1998).
[26] Goth, L., *Clin. Chim. Acta* **143** (1991).

[27] Packer, L. and Glazer, A. N., *Methods in Enzymology* **186** (1990).
[28] Vowells, S. J., Sekhsaria, S., Malech, H. L., Shalit, M. and Fleisher, T. A., *J. Immunol. Methods* **178**, 89 (1995).
[29] Pick, E. and Mizel, D. J., *Immunol. Methods* **46**, 211 (1981).
[30] Miyasaka, C. K., Souza, J. A. A., Pires de Melo, M., Pithon Curi, T. C., Lajolo, F. M. and Curi, R., *Gen. Pharmac.* **31**, 37 (1998).
[31] Hosker, H. S., Kelly, C. and Corris, P. A., *Blood Rev.* **3**, 88 (1989).
[32] Baier, R. E. and Meyer, A. E., *J. Dent. Ed.* **52**, 788 (1988).
[33] Meyer, A. E., Baier, R. E., Natiella, J. R. and Meenaghan, M. A., *J. Oral Implantol.* **14**, 363 (1988).
[34] Baier, R. E., Natiella, J. R., Meyer, A. E. and Carter, J. M., *Tissue Integration in Oral and Maxillo-Facial Reconstruction* (Excerpta Medica, Amsterdam, 1986), pp. 13–40.